Inorganica Chimica Acta 384 (2012) 333–339

Contents lists available at SciVerse ScienceDirect

Inorganica Chimica Acta

journal homepage: www.elsevier.com/locate/ica

First lanthanide coordination polymers with *N*,*N*-dimethylformamide hydrolysis induced formate ligands

Guang Huang [a], Ping Yang [a,b], Ning Wang [c], Jian-Zhong Wu [a,*], Ying Yu [a]

[a] School of Chemistry and Environment, South China Normal University, Guangzhou 510006, China
[b] School of Chemistry and Chemical Engineering, Sun Yat-Sen University, Guangzhou 510631, China
[c] Research Institute of Tsinghua University in Shenzhen, Shenzhen 518055, China

ARTICLE INFO

Article history:
Received 9 May 2011
Received in revised form 16 November 2011
Accepted 15 December 2011
Available online 26 December 2011

Keywords:
Lanthanide
Carboxylate
Hydrolysis
Crystal structure
Photoluminescence
Magnetism

ABSTRACT

A series of isostructural lanthanide organic frameworks with composition [Ln(tpa)(fa)] (Ln = Eu, Gd, Tb; H_2tpa = terephthalic acid, i.e. 1,4-benzenedicarboxylic acid; Hfa = formic acid, i.e. methanoic acid) has been synthesized through reaction of the corresponding lanthanide nitrates with H_2tpa in DMF/H_2O mixed solvent under solvothermal conditions (DMF = *N*,*N*-dimethylformamide). The formate ligand is in situ generated by hydrolysis of DMF. The dilanthanide-diformate subunits build two-dimensional layers which are shored up by terephthalates, leading to a three-dimensional pillar-layer network. These are the first examples of lanthanide complexes containing the formate ligand originated from hydrolysis of DMF. The dilanthanide-diformate subunit is also the first ever reported. The Eu and Tb complexes emit strong ligand sensitized f–f luminescence. Temperature variable magnetic susceptibility analysis reveals that the Gd(III) atoms are antiferromagnetically coupled ($J = -0.0048\ \mathrm{cm}^{-1}$, $\hat{H} = -2J\hat{S}_{\mathrm{Gd1}}\cdot\hat{S}_{\mathrm{Gd2}}$).

1. Introduction

Research on synthesis and characterization of metal organic coordination polymeric materials has attracted continuous interests for their potential applications and esthetic beauty associated with the network structures [1–3]. The use of lanthanide salts and organic linkers in the synthesis of polymeric materials has gained much attention due to their unique photophysical and magnetic properties, although lack of preferred coordination number and geometry for lanthanide ions makes it difficult to predict the structure of the lanthanide coordination polymers. Choice of organic linkers is essential for preparing novel lanthanide organic polymers. The hard Lewis base nature of multicarboxylate-containing ligands makes them suitable for connecting the lanthanide ions [4].

Terephthalic acid (H_2tpa, 1,4-benzenedicarboxylic acid) has drawn much attention in preparing lanthanide coordination polymers, because its two carboxylate groups after double deprotonation have a good affinity for lanthanide ions, and its rod-like topology induces low steric hindrance, allowing formation of porous frameworks [5–16]. Based on terephthalate and other ligands, numerous mixed-ligand lanthanide complexes have been prepared. It has been found that the reaction conditions have significant influence on the structures of the final products. As regards the lanthanide–terephthalate systems involving DMF (*N*,*N*-dimethylformamide), it was firstly reported that standing the DMF/methanol solution of terbium nitrate with terephthalic acid in pyridine vapor at room temperature yielded microporous Tb(tpa)(NO_3)(DMF)$_2$ where DMF and nitrate were also ligated [6]. In another paper, microporous frameworks Tb_3(tpa)$_{4.5}$(DMF)$_2$(H_2O)$_3$·(DMF)(H_2O) and Ln_3(tpa)$_{4.5}$(DMF)$_2$(H_2O)$_3$·(DMF)(H_2O)$_{0.5}$(C_2H_5OH)$_{0.5}$ (Ln = Dy, Ho, Er) were synthesized by the reaction of lanthanide nitrates with H_2tpa and triethylenetetramine in a mixed solution of DMF, water and ethanol at 55 °C [12]. Ln_6(tpa)$_9$(DMF)$_6$(H_2O)$_3$·3DMF (Ln = La, Ce, Nd) or Ln_2(tpa)$_3$(DMF)$_2$(H_2O)$_2$ (Ln = Y, Dy, Eu) were obtained by slow diffusion of the solution of Ln(NO_3)$_3$·6H_2O in DMF/H_2O into the solution containing Na_2tpa in DMF/H_2O [14]. No study of the reactions involving the relevant reactants under hydro(solvo)thermal conditions were reported.

The hydro(solvo)thermal process provides a supercritical environment with simultaneous high temperature and high pressure and has been widely utilized recently in the synthesis of highly stable and solvent insoluble coordination polymeric materials. However, it is still a great challenge to control the products. Further studies are needed to understand the mechanism and discipline in hydro(solvo)thermal reactions. It is interesting that in hydro(solvo)thermal conditions, some unique in situ reactions involving the organic ligands may happen which seem to unlikely occur in normal conditions [17–19]. This makes the

---

* Corresponding author. Tel.: +86 20 31759373; fax: +86 20 85211642.
E-mail address: wujzh@scnu.edu.cn (J.-Z. Wu).

0020-1693/$ - see front matter © 2011 Elsevier B.V. All rights reserved.
doi:10.1016/j.ica.2011.12.030

hydro(solvo)thermal synthesis a fascinating method to obtain novel coordination polymers.

Based on the above considerations, we investigated the reaction of lanthanide nitrates with H_2tpa in DMF/H_2O under hydro(solvo) thermal conditions. Interestingly, an unexpected series of coordination polymers with composition [Ln(tpa)(fa)] (Ln = Eu, Gd, Tb; fa = formate, i.e. methanoate) were obtained, where the ligand formate is the hydrolysate of DMF. To the best of our knowledge, these compounds represent the first lanthanide complexes containing formate originated from hydrolysis of DMF.

2. Experimental

2.1. Materials and measurements

$Ln(NO_3)_3 \cdot 6H_2O$ (Ln = Eu, Tb, Gd) were prepared by dissolving the corresponding Ln_2O_3 in 1:1 nitric acid and then evaporating the solvent to dryness. DMF was distilled and stored over molecular sieves. All the other reagents commercially available were used without further purification. Elemental analysis results were obtained on a Thermo Electron Flash EA 1112 Elemental Analyzer. The luminescence spectra were recorded with a Hitachi F2500 Fluorescence Spectrophotometer. The magnetic susceptibility measurement was carried out for polycrystalline samples on a Quantum Design MPMS-XL5 SQUID magnetometer. Powder X-ray diffraction (PXRD) patterns were recorded on a Rigaku D/M-2200T automated diffractometer for Cu Kα radiation (λ = 1.54056 Å), with a scan speed of 4°/min and a step size of 0.02° in the 2θ range of 5–50°.

2.2. Synthesis

The complexes [Ln(tpa)(fa)] (Ln = Eu, **1**; Gd, **2**; Tb, **3**) were synthesized similarly as follows. The corresponding lanthanide nitrate (0.2 mmol) and H_2tpa (0.2 mmol) dissolved in a mixture of DMF (4 mL) and water (6 mL) in a 23 mL Teflon-lined stainless steel reactor was heated at 160 °C for 72 h. The reaction system was cooled at a speed of 5 °C/h to room temperature. Block crystals were collected and washed with distilled water, yields around 65% based on the lanthanide metals. Microanalysis: Calc. for $C_9H_5O_6Eu$: C, 29.93; H, 1.40. Found: C, 29.97; H, 1.38%. Calc. for $C_9H_5O_6Gd$: C, 29.50; H, 1.38. Found: C, 29.48; H, 1.42%. Calc. for $C_9H_5O_6Tb$: C, 29.37; H, 1.36. Found: C, 29.64; H, 1.51%.

2.3. X-ray crystallography

Single crystals of complexes were carefully selected under a microscope and glued at the tip of a thin glass fiber with cyanoacrylate adhesive. X-ray diffraction was performed on a Bruker Apex-II CCD X-ray diffractometer with Mo Kα radiation operating at 50 kV and 30 mA. The crystal structures were solved by direct method and refined on F^2 by full-matrix least-squares method. All non-hydrogen atoms were refined anisotropically. All the H atoms for organic ligand were placed at the calculation positions. Further details of the X-ray structural analysis are given in Table 1.

3. Results and discussion

3.1. Synthesis

DMF is a frequently used solvent in preparing coordination compounds. But it could occasionally hydrolyze in acidic solution, under either normal or solvothermal conditions, giving rise to the dimethylammonium cation [20–31] or sometimes the formate anion [32–35] as a component in the final complexes. To the best of our knowledge, there is no report involving any lanthanide complex with formate originated from hydrolysis of DMF, although a few lanthanide complexes containing DMF generated dimethylammonium have been reported recently [36–38]. The three lanthanide complexes reported here represent the first examples of lanthanide complexes with DMF generated formate ligand. It is some interesting that when we used formic acid in place of DMF, the product yields decreased vastly (less than 5%), which implies that the slow hydrolysis of DMF may be important for the product formation.

3.2. Structural description

The single crystallographic analysis reveals that complexes **1**, **2** and **3** are isostructural. As can be seen in Table 1, the crystal cell size decreases on going from Eu to Gd and to Tb, which is consistent with the lanthanide contraction effect. The variation of the corresponding bond lengths as listed in Table 2 also provide direct criteria for lanthanide contraction. In order to assist the explanation of the magnetic property of the Gd complex **2** as will be discussed later, the structure of **2** is described here in detail. As displayed in Fig. 1, a Gd(III) atom is eight-coordinated by four O atoms each from a tpa^{2-} ligand and four O atoms from three fa^- ligand. The Gd–O bond lengths (Table 2) for O5 and O6 atoms of formate [2.383(3)–2.578(3) Å] are significantly longer than those for O1, O2, O3 and O4 atoms of terephthalate [2.279(3)–2.346(3) Å]. This can be explained by that the formate ligand forms an unstable four-membered chelate ring with the gadolinium atom. As illustrated in Scheme 1, both terephthalate and formate function as bridging ligands in the present complexes, connecting four and three lanthanide atoms, respectively. But only the formate plays also as a chelator here. The non-chelation tetradentate binding mode of terephthalate in Scheme 1 is commonly seen in other lanthanide–terephthalate systems [5–7,12–14,16]. Other binding modes of terephthalate involving four-membered chelation ring formation [8–12,14–16] are not existed in the present complexes.

The continuous linkage between the formate ligands and the Gd(III) atoms forms a two-dimensional layer. One can also regard the layer as being built by alternately connected centrosymmetric Gd_2fa_2 dimeric subunits, as emphasized by the circle shown in Fig. 2. Such dilanthanide-diformate units are the first reported examples to date. The Gd···Gd distance, 3.9566(3) Å, is shorter than those in other digadolinium-dicarboxylate units [39–60], ascribable to smaller steric hindrance of formate than other carboxylates. The Gd_2O_2 diamonds are evenly separated by 7.2866(4) Å, forming a rhombic (4,4) grid network. The parallel layers are overlapped if viewing down the *a* axis.

All the terephthalate ligands incline between the layers. For each terephthalate ligand, two O atoms in a carboxylate group connect two Gd(III) atoms in the same Gd_2O_2 diamond in one layer, while the two O atoms in the para-carboxylate group link two Gd(III) atoms which come from two adjacent Gd_2O_2 diamonds. The interlayer distance is 10.8849(8) Å. So the terephthalate ligands function like pillars to shore up the layers, resulting in three-dimensional “pillar-layer” network, as shown in Fig. 3. Such pillar-layer network is quite compact and no remarkable porosity is existed.

3.3. Bulky purity and photoluminescence properties

The purity of the bulky products of the complexes was confirmed by elemental analysis (see Section 2) and powder X-ray diffraction. As shown in Fig. 4, the room temperature diffraction patterns of the europium complex **1** as synthesized are in good agreement with the calculated diffractogram based on the single crystal data, implying that the bulky sample is phase pure. The

Table 1
Crystal data and structure refinement.

Complex	1	2	3
Empirical formula	$C_9H_5EuO_6$	$C_9H_5GdO_6$	$C_9H_5O_6Tb$
Formula weight	361.09	366.38	368.05
T (K)	298(2)	298(2)	298(2)
λ (Å)	0.71073	0.71073	0.71073
Crystal system	monoclinic	monoclinic	monoclinic
Space group	$P2_1/c$	$P2_1/c$	$P2_1/c$
Unit cell dimensions			
a (Å)	10.6699(13)	10.6678(8)	10.6621(9)
b (Å)	12.9403(16)	12.9319(9	12.8903(11)
c (Å)	6.7635(8)	6.7191(5)	6.7157(6)
β (°)	95.4450(10)	95.2900	95.2710
Volume (Å^3)	929.6(2)	922.98(12)	918.9(14)
Z	4	4	4
Density (Mg m^{-3})	2.580	2.637	2.660
μ (mm^{-1})	6.756	7.195	7.705
F(000)	680	684	688
Reflections collected	5004	4938	4779
Independent reflections	1819	1805	1703
R_{int}	0.0187	0.0234	0.0184
Goodness-of-fit (GOF) on F^2	1.128	0.959	1.018
R_1, wR_2 [$I > 2\sigma(I)$]	0.0204, 0.0445	0.0209, 0.0549	0.0222, 0.0506
R_1, wR_2 (all data)	0.0229, 0.0453	0.0230, 0.0563	0.0243, 0.0516

Table 2
Bond lengths (Å) and angles (°).

1		2		3	
Eu(1)–O(1)$^{\#1}$	2.335(3)	Gd(1)–O(1)$^{\#1}$	2.333(3)	Tb(1)–O(1)$^{\#1}$	2.330(3)
Eu(1)–O(2)	2.285(3)	Gd(1)–O(2)	2.279(3)	Tb(1)–O(2)	2.272(3)
Eu(1)–O(3)$^{\#2}$	2.321(3)	Gd(1)–O(3)$^{\#2}$	2.311(3)	Tb(1)–O(3)$^{\#2}$	2.313(3)
Eu(1)–O(4)$^{\#3}$	2.354(3)	Gd(1)–O(4)$^{\#3}$	2.346(3)	Tb(1)–O(4)$^{\#3}$	2.352(4)
Eu(1)–O(5)	2.574(3)	Gd(1)–O(5)	2.554(3)	Tb(1)–O(5)	2.558(4)
Eu(1)–O(5)$^{\#4}$	2.471(3)	Gd(1)–O(5)$^{\#4}$	2.470(3)	Tb(1)–O(5)$^{\#4}$	2.462(3)
Eu(1)–O(6)	2.588(3)	Gd(1)–O(6)	2.578(3)	Tb(1)–O(6)	2.575(4)
Eu(1)–O(6)$^{\#5}$	2.392(3)	Gd(1)–O(6)$^{\#5}$	2.383(3)	Tb(1)–O(6)$^{\#5}$	2.383(4)
O(1)$^{\#1}$–Eu(1)–O(4)$^{\#3}$	145.44(10)	O(1)$^{\#1}$–Gd(1)–O(4)$^{\#3}$	144.99(10)	O(1)$^{\#1}$–Tb(1)–O(4)$^{\#3}$	145.49(12)
O(1)$^{\#1}$–Eu(1)–O(5)	80.59(9)	O(1)$^{\#1}$–Gd(1)–O(5)	80.44(9)	O(1)$^{\#1}$–Tb(1)–O(5)	80.69(11)
O(1)$^{\#1}$–Eu(1)–O(5)$^{\#4}$	75.26(9)	O(1)$^{\#1}$–Gd(1)–O(5)$^{\#4}$	75.10(10)	O(1)$^{\#1}$–Tb(1)–O(5)$^{\#4}$	75.33(12)
O(1)$^{\#1}$–Eu(1)–O(6)	122.55(10)	O(1)$^{\#1}$–Gd(1)–O(6)	122.75(9)	O(1)$^{\#1}$–Tb(1)–O(6)	122.69(12)
O(1)$^{\#1}$–Eu(1)–O(6)$^{\#5}$	135.83(10)	O(1)$^{\#1}$–Gd(1)–O(6)$^{\#5}$	136.25(10)	O(1)$^{\#1}$–Tb(1)–O(6)$^{\#5}$	135.83(12)
O(2)–Eu(1)–O(1)$^{\#1}$	78.24(10)	O(2)–Gd(1)–O(1)$^{\#1}$	77.92(10)	O(2)–Tb(1)–O(1)$^{\#1}$	78.06(12)
O(2)–Eu(1)–O(3)$^{\#2}$	100.30(10)	O(2)–Gd(1)–O(3)$^{\#2}$	100.08(11)	O(2)–Tb(1)–O(3)$^{\#2}$	100.05(13)
O(2)–Eu(1)–O(4)$^{\#3}$	101.34(11)	O(2)–Gd(1)–O(4)$^{\#3}$	101.72(12)	O(2)–Tb(1)–O(4)$^{\#3}$	101.59(13)
O(2)–Eu(1)–O(5)	157.01(9)	O(2)–Gd(1)–O(5)	156.42(9)	O(2)–Tb(1)–O(5)	156.93(11)
O(2)–Eu(1)–O(5)$^{\#4}$	77.24(9)	O(2)–Gd(1)–O(5)$^{\#4}$	77.07(9)	O(2)–Tb(1)–O(5)$^{\#4}$	77.41(12)
O(2)–Eu(1)–O(6)	152.80(9)	O(2)–Gd(1)–O(6)	152.91(9)	O(2)–Tb(1)–O(6)	152.78(11)
O(2)–Eu(1)–O(6)$^{\#5}$	78.44(10)	O(2)–Gd(1)–O(6)$^{\#5}$	78.62(10)	O(2)–Tb(1)–O(6)$^{\#5}$	78.53(12)
O(3)$^{\#2}$–Eu(1)–O(1)$^{\#1}$	76.23(10)	O(3)$^{\#2}$–Gd(1)–O(1)$^{\#1}$	76.35(10)	O(3)$^{\#2}$–Tb(1)–O(1)$^{\#1}$	76.13(12)
O(3)$^{\#2}$–Eu(1)–O(4)$^{\#3}$	136.35(10)	O(3)$^{\#2}$–Gd(1)–O(4)$^{\#3}$	136.61(10)	O(3)$^{\#2}$–Tb(1)–O(4)$^{\#3}$	136.39(12)
O(3)$^{\#2}$–Eu(1)–O(5)	83.14(10)	O(3)$^{\#2}$–Gd(1)–O(5)	83.68(10)	O(3)$^{\#2}$–Tb(1)–O(5)	83.36(13)
O(3)$^{\#2}$–Eu(1)–O(5)$^{\#4}$	151.28(10)	O(3)$^{\#2}$–Gd(1)–O(5)$^{\#4}$	151.26(10)	O(3)$^{\#2}$–Tb(1)–O(5)$^{\#4}$	151.24(12)
O(3)$^{\#2}$–Eu(1)–O(6)	71.51(10)	O(3)$^{\#2}$–Gd(1)–O(6)	71.65(10)	O(3)$^{\#2}$–Tb(1)–O(6)	71.71(13)
O(3)$^{\#2}$–Eu(1)–O(6)$^{\#5}$	71.76(10)	O(3)$^{\#2}$–Gd(1)–O(6)$^{\#5}$	72.10(10)	O(3)$^{\#2}$–Tb(1)–O(6)$^{\#5}$	71.78(13)
O(4)$^{\#3}$–Eu(1)–O(5)	91.06(11)	O(4)$^{\#3}$–Gd(1)–O(5)	90.69(11)	O(4)$^{\#3}$–Tb(1)–O(5)	90.88(13)
O(4)$^{\#3}$–Eu(1)–O(5)$^{\#4}$	71.06(9)	O(4)$^{\#3}$–Gd(1)–O(5)$^{\#4}$	70.84(10)	O(4)$^{\#3}$–Tb(1)–O(5)$^{\#4}$	71.05(12)
O(4)$^{\#3}$–Eu(1)–O(6)	71.94(10)	O(4)$^{\#3}$–Gd(1)–O(6)	71.88(11)	O(4)$^{\#3}$–Tb(1)–O(6)	71.75(13)
O(4)$^{\#3}$–Eu(1)–O(6)$^{\#5}$	76.10(10)	O(4)$^{\#3}$–Gd(1)–O(6)$^{\#5}$	76.08(10)	O(4)$^{\#3}$–Tb(1)–O(6)$^{\#5}$	76.07(13)
O(5)$^{\#4}$–Eu(1)–O(5)	88.83(5)	O(5)$^{\#4}$–Gd(1)–O(5)	88.45(5)	O(5)$^{\#4}$–Tb(1)–O(5)	88.64(7)
O(5)$^{\#4}$–Eu(1)–O(6)	122.48(9)	O(5)$^{\#4}$–Gd(1)–O(6)	122.63(9)	O(5)$^{\#4}$–Tb(1)–O(6)	122.35(12)
O(5)–Eu(1)–O(6)	49.80(9)	O(5)–Gd(1)–O(6)	50.30(9)	O(5)–Tb(1)–O(6)	49.90(11)
O(6)$^{\#5}$–Eu(1)–O(5)	123.71(9)	O(6)$^{\#5}$–Gd(1)–O(5)	124.22(9)	O(6)$^{\#5}$–Tb(1)–O(5)	123.70(11)
O(6)$^{\#5}$–Eu(1)–O(5)$^{\#4}$	133.82(10)	O(6)$^{\#5}$–Gd(1)–O(5)$^{\#4}$	133.41(9)	O(6)$^{\#5}$–Tb(1)–O(5)$^{\#4}$	133.85(12)
O(6)$^{\#5}$–Eu(1)–O(6)	74.36(11)	O(6)$^{\#5}$–Gd(1)–O(6)	74.29(10)	O(6)$^{\#5}$–Tb(1)–O(6)	74.25(13)

Symmetry transformations used to generate equivalent atoms: #1, x, $-y + 3/2$, $z - 1/2$; #2, $-x$, $-y + 2$, $-z$; #3, $x + 1$, y, z; #4, x, $-y + 3/2$, $z + 1/2$; #5, $-x + 1$, $-y + 2$, $-z$.

pure crystalline samples are thus suitable for studies of photoluminescent and magnetic properties.

Photoluminescence is one of important properties of the lanthanide complexes with aromatic ligands since a highly absorptive ligand may sensitize the f–f transition of the lanthanide atom. The emission spectra, especially the environment relevant transitions of the Eu(III) atom provide important structural information [61]. As depicted in Fig. 5, the ligand-centered luminescence is completely suppressed, whereas the typical narrow emission bands of the Eu(III) or Tb(III) ions can be detected upon excitation of

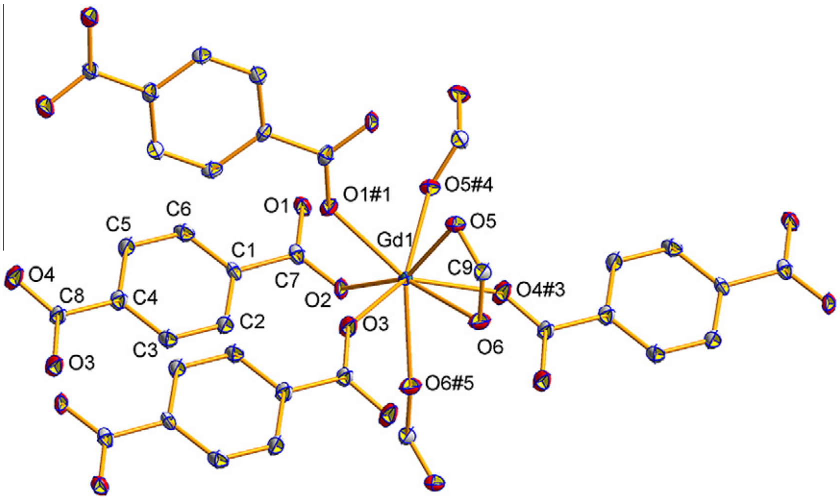

Fig. 1. ORTEP plot (50% thermal ellipsoids) of the coordination environment around a Gd(III) atom in **2** with atom labeling. All hydrogen atoms are omitted for clarity. Symmetry codes: #1, *x*, −*y* + 3/2, *z* − 1/2; #2, −*x*, −*y* + 2, −*z*; #3, *x* + 1, *y*, *z*; #4, *x*, −*y* + 3/2, *z* + 1/2; #5, −*x* + 1, −*y* + 2, −*z*.

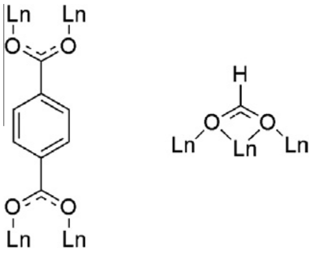

Scheme 1. Binding modes of terephthalate (left) and formate (right) in **1**, **2** and **3**.

the ligand-centered absorption at 317 nm, showing strong ligand sensitized f–f emission. For the europium complex **1** (Fig. 5a), the presence of the weak unsplit $^5D_0 \rightarrow {}^7F_0$ electric-dipole transition indicates only one type of europium site and the site symmetry is not especially high (i.e. the europium atom is not on an inversion centre). The doublet $^5D_0 \rightarrow {}^7F_1$ transition (magnetic-dipole allowed and relatively insensitive to environment) also reflects a low symmetry environment. The hypersensitive $^5D_0 \rightarrow {}^7F_2$ electric dipole transition was found to be the strongest emission and split to two or three peaks (the 616 nm peak not resolved well), strongly supporting that the central europium ion locates at site in low symmetry without inversion centre. These features agree well with the X-ray structural analysis as discussed above.

In contrast to the bright red emission of **1**, the terbium complex **3** displays bright green luminescence, with emission peaks centered at 489 nm ($^5D_4 \rightarrow {}^7F_6$), 546 nm ($^5D_4 \rightarrow {}^7F_5$), 584 nm ($^5D_4 \rightarrow {}^7F_4$), 622 nm ($^5D_4 \rightarrow {}^7F_3$) (Fig. 5b). The slight splitting of these peaks also verifies the low symmetry around the terbium atoms.

3.4. Magnetic property

As Gd(III) has the largest spin among the lanthanide ions, it is worthy to study the magnetic behavior of the Gd(III) complex.

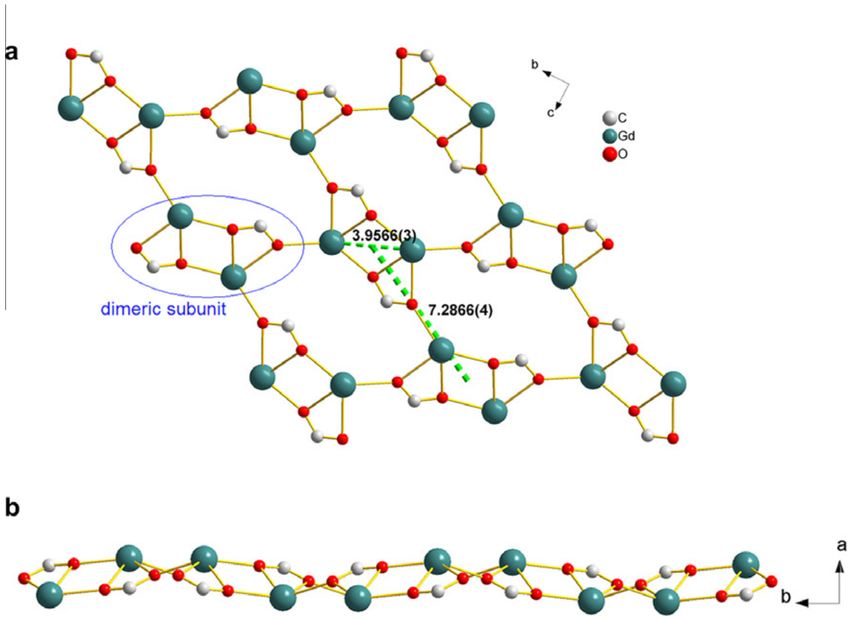

Fig. 2. Two-dimensional layer formed by formates and Gd(III) atoms in **2**. (a) Projection down the *a* axis showing the (4,4) net. (b) View as a layer down the *c* axis.

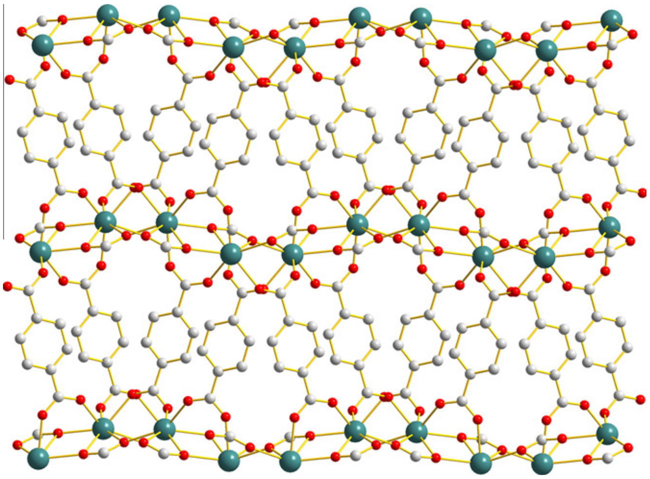

Fig. 3. Projection down the *c* axis, showing the three dimensional pillar-layer network in **2** with terephthalates shoring up the Gd-formate layers.

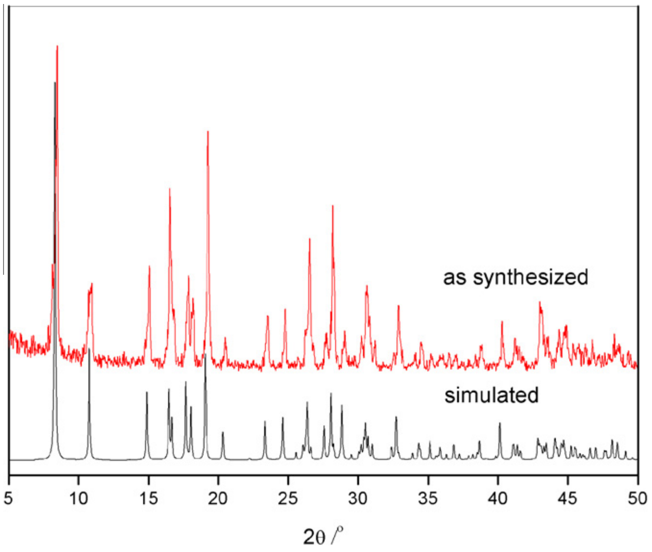

Fig. 4. The experimental and simulated PXRD patterns of **1** at room temperature.

The temperature variable magnetic susceptibility measurement for the gadolinium complex **2** was performed in the range of 2–300 K under a field of 1000 Oe, and the magnetic behavior is shown in Fig. 6 as plots of $\chi_M{}^{-1}$ vs. T and $\chi_M T$ vs. T, where χ_M is the magnetic susceptibility per mononuclear Gd unit.

The thermal evolution of $\chi_M{}^{-1}$ obeys Curie–Weiss law, $\chi_M = C/(T - \theta)$, over the whole temperature range with Curie constant $C = 7.995\ \mathrm{cm^3\ mol^{-1}\ K}$ and Weiss constant $\theta = -0.411$ K. The small negative value of the Weiss constant implies the weak antiferromagnetic coupling between the Gd(III) ions.

The $\chi_M T$ value at room temperature is $7.98\ \mathrm{cm^3\ mol^{-1}\ K}$, close to the expected value for an uncoupled Gd(III) ion with ${}^8S_{7/2}$ ground state ($7.88\ \mathrm{cm^3\ mol^{-1}\ K}$, $g = 2$). With the decreasing of temperature, $\chi_M T$ decreases slowly till about 10 K and then drops sharply to $7.08\ \mathrm{cm^3\ mol^{-1}\ K}$ at 2 K. This is a typical behavior for weak antiferromagnetic interaction, consistent with the indication of the Weiss constant.

As can be seen from the structural details discussed above, the magnetic coupling of the Gd(III) ions is mainly realized through the dimeric Gd_2O_2 unit which has a short Gd⋯Gd distance, 3.9566(3) Å. The magnetic interaction between the formate connected intra-layer Gd_2O_2 units with even distance 7.2866(4) Å (Fig. 2) is also possible, whereas the magnetic interaction between the terephthalate connected inter-layer Gd_2O_2 units with long distance 10.8849(8) Å is negligible.

For the Gd_2O_2 diamond system, the simple dimer model based on spin Hamitonian $\hat{H} = -2J\hat{S}_{Gd1}\cdot\hat{S}_{Gd2}$ with quantum numbers

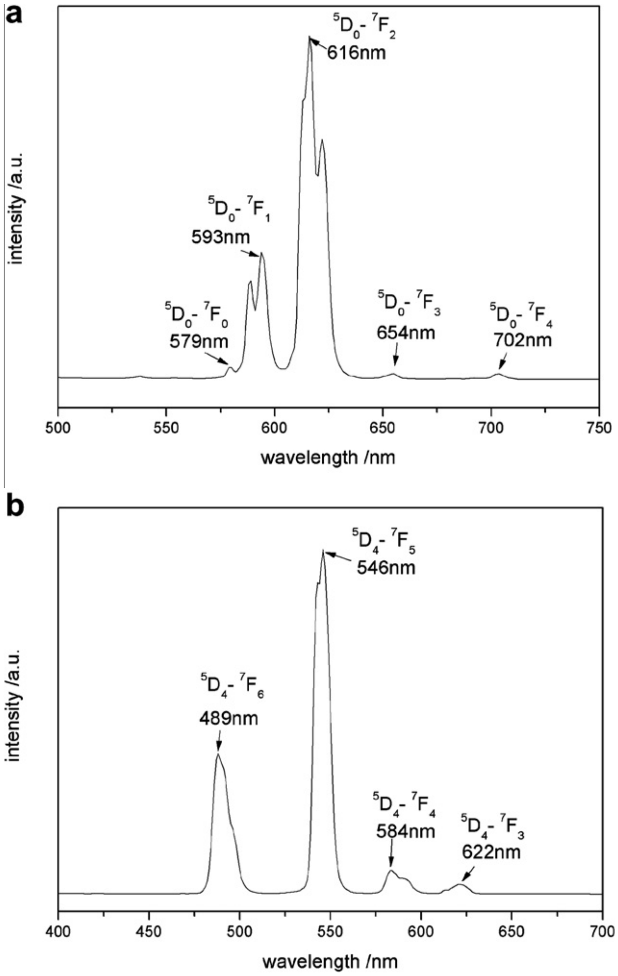

Fig. 5. Solid-state emission spectra of **1** (a) and **3** (b) at room temperature. $\lambda_{ex} = 317$ nm.

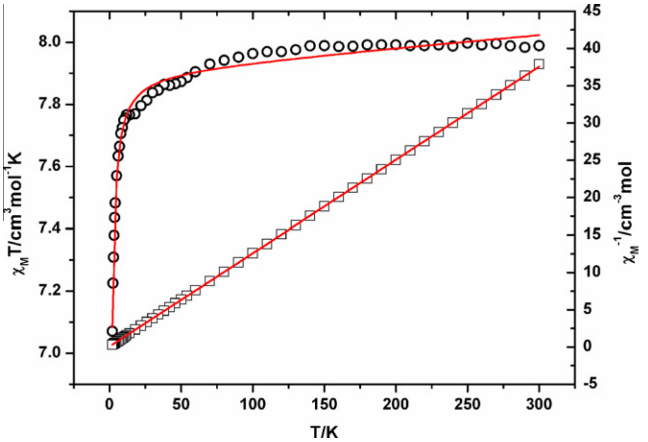

Fig. 6. $\chi_M{}^{-1}$ vs. T and $\chi_M T$ vs. T plots for **2**.

$S_{Gd1} = S_{Gd2} = 7/2$, as reported previously [62–66], can be used here. The molar magnetic susceptibility can be expressed as

$$\chi'_M = \frac{Ng^2\beta^2}{3k_BT} \cdot \frac{6e^{\frac{2J}{k_BT}} + 30e^{\frac{6J}{k_BT}} + 84e^{\frac{12J}{k_BT}} + 180e^{\frac{20J}{k_BT}} + 330e^{\frac{30J}{k_BT}} + 546e^{\frac{42J}{k_BT}} + 840e^{\frac{56J}{k_BT}}}{1 + 3e^{\frac{2J}{k_BT}} + 5e^{\frac{6J}{k_BT}} + 7e^{\frac{12J}{k_BT}} + 9e^{\frac{20J}{k_BT}} + 11e^{\frac{30J}{k_BT}} + 13e^{\frac{42J}{k_BT}} + 15e^{\frac{56J}{k_BT}}}$$

where N, β, k_B, g, J and T have their usual meanings. Considering the two-dimensional square lattice coupling [67,68], the magnetic susceptibility can be further rewritten as

$$\chi_M = \frac{Ng^2\beta^2}{3k_BT} \cdot S(S+1) \cdot \frac{(1+u)^2}{(1-u)^2} + \text{TIP}$$

$$S(S+1) = \chi'_M \cdot \frac{Ng^2\beta^2}{3k_BT}$$

$$u = \coth\frac{J_1S(S+1)}{k_BT} - \frac{k_BT}{J_1S(S+1)}$$

where J_1 and TIP represent the magnetic exchange parameter between the adjacent Gd_2O_2 diamonds and temperature-independent paramagnetism, respectively. The best fitting result is $g = 2.00$, $J = -0.0048\ \text{cm}^{-1}$, $J_1 = -0.0025\ \text{cm}^{-1}$, $\text{TIP} = 8.04 \times 10^{-4}\ \text{cm}^3\ \text{mol}^{-1}$ and R (residue sum of squares) = 4.99×10^{-4}. The very small negative values of the coupling constants indicate very weak antiferromagnetic interaction between the Gd(III) ions.

Recently the magneto-structural studies of oxo-carboxylate bridged Gd(III) complexes have made remarkable progress [66,69–72]. It has been found that there is a strong relationship between a certain bridging motif and the magnetic exchange interaction [66,69,72]. The structural data for the Gd_2O_2 diamond, especially the Gd–O–Gd angle or the Gd···Gd distance, seem to have crucial effect on the computed magnetic coupling parameters. Based on structural and magnetic data for a number of oxo-carboxylate bridged Gd(III) complexes, Ruiz-Pérez and her coworkers have compiled a detailed table for comparison and concluded that the Gd–O–Gd angle smaller than 110° may lead to an antiferromagnetic behavior [69]. The bridging motif in a dimeric unit of **2** is shown in Fig. 7, with two μ-carboxylato-κ^1O:κ^1O' groups from terephthalate ligands and two μO:κ^2O,O' formate ligands as the bridges. The Gd–O–Gd angle is 105.7(1)°, less than 110°. The Gd···Gd distance, 3.9566(3) Å, is among the smallest ones in the Gd_2O_2 cores. Such "compact" digadolinium structure favors significant increasing of the overlap integral of the magnetic orbitals and thus the weak antiferromagnetic contribution to the exchange coupling.

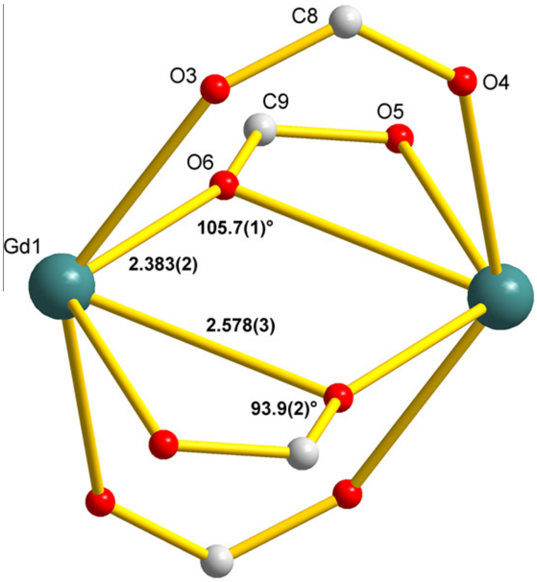

Fig. 7. The centrosymmetric bridging motif in **2**.

4. Conclusions

The reactions of europium, gadolinium or terbium nitrates with terephthalic acid in DMF/H_2O at solvothermal conditions yielded three new isostructural coordination polymers with mixed terephthalate and formate ligands. These complexes represent the first lanthanide complexes containing the formate ligand originated from hydrolysis of DMF. The dilanthanide-diformate dimeric unit is also the first ever found in literature. The connection of these dimeric units constitute (4,4) layers which are shored up by terephthalates. The europium and terbium complexes possess ligand sensitized red and green luminescence, respectively. The gadolinium complex shows a weak antiferromagnetic behavior between the Gd(III) ions due to the bridging motif with small Gd–O–Gd angle and Gd···Gd distance involving the dimeric unit.

Acknowledgments

Financial supports from the National Natural Science Foundation (20975041), Guangdong Natural Science Foundation (5005935) and South China Normal University are gratefully acknowledged.

Appendix A. Supplementary material

CCDC 820774, 820775 and 820776 contain the supplementary crystallographic data for the complexes **1**, **2** and **3**. These data can be obtained free of charge from The Cambridge Crystallographic Data Centre via www.ccdc.cam.ac.uk/data_request/cif. Supplementary data associated with this article can be found, in the online version, at doi:10.1016/j.ica.2011.12.030.

References

[1] A.U. Czaja, N. Trukhan, U. Muller, Chem. Soc. Rev. 38 (2009) 1284.
[2] L.Q. Ma, C. Abney, W.B. Lin, Chem. Soc. Rev. 38 (2009) 1248.
[3] D.J. Tranchemontagne, J.L. Mendoza-Cortes, M. O'Keeffe, O.M. Yaghi, Chem. Soc. Rev. 38 (2009) 1257.
[4] D.T. De Lill, C.L. Cahill, Prog. Inorg. Chem. 55 (2007) 143.
[5] T.M. Reineke, M. Eddaoudi, M. Fehr, D. Kelley, O.M. Yaghi, J. Am. Chem. Soc. 121 (1999) 1651.
[6] T.M. Reineke, M. Eddaoudi, M. O'Keeffe, O.M. Yaghi, Angew. Chem., Int. Ed. 38 (1999) 2590.
[7] L. Pan, N. Zheng, Y. Wu, S. Han, R. Yang, X. Huang, J. Li, Inorg. Chem. 40 (2001) 828.
[8] C. Serre, F. Millange, J. Marrot, G. Férey, Chem. Mater. 14 (2002) 2409.
[9] A. Deluzet, W. Maudez, C. Daiguebonne, O. Guillou, Cryst. Growth Des. 3 (2003) 475.
[10] B. Chen, Y. Yang, F. Zapata, G. Qian, Y. Luo, J. Zhang, E.B. Lobkovsky, Inorg. Chem. 45 (2006) 8882.
[11] C. Daiguebonne, N. Kerbellec, K. Bernot, Y. Gérault, A. Deluzet, O. Guillou, Inorg. Chem. 45 (2006) 5399.
[12] X. Guo, G. Zhu, F. Sun, Z. Li, X. Zhao, X. Li, H. Wang, S. Qiu, Inorg. Chem. 45 (2006) 2581.
[13] D. Weng, X. Zheng, L. Jin, Eur. J. Inorg. Chem. 2006 (2006) 4184.
[14] Y. Han, X. Li, L. Li, C. Ma, Z. Shen, Y. Song, X. You, Inorg. Chem. 49 (2010) 10781.
[15] H. He, D. Yuan, H. Ma, D. Sun, G. Zhang, H.-C. Zhou, Inorg. Chem. 49 (2010) 7605.
[16] R.A. Zehnder, R.A. Renn, E. Pippin, M. Zeller, K.A. Wheeler, J.A. Carr, N. Fontaine, N.C. McMullen, J. Mol. Struct. 985 (2011) 109.
[17] X.M. Zhang, Coord. Chem. Rev. 249 (2005) 1201.
[18] X.M. Chen, M.L. Tong, Acc. Chem. Res. 40 (2007) 162.
[19] H. Zhao, Z.R. Qu, H.Y. Ye, R.G. Xiong, Chem. Soc. Rev. 37 (2008) 84.
[20] C.A. Murphy, T.S. Cameron, M.W. Cooke, M.A.S. Aquino, Inorg. Chim. Acta 305 (2000) 225.

[21] W. Chen, J.-Y. Wang, C. Chen, Q. Yue, H.-M. Yuan, J.-S. Chen, S.-N. Wang, Inorg. Chem. 42 (2003) 944.
[22] E. Kahrovic, P. Orioli, B. Bruni, M. Di Vaira, L. Messori, Inorg. Chim. Acta 355 (2003) 420.
[23] S.V. Ganesan, P. Lightfoot, S. Natarajan, Solid State Sci. 6 (2004) 757.
[24] G.S. Papaefstathiou, S. Manessi, C.P. Raptopoulou, E.J. Behrman, T.F. Zafiropoulos, Inorg. Chem. Commun. 7 (2004) 69.
[25] A.D. Burrows, K. Cassar, R.M.W. Friend, M.F. Mahon, S.P. Rigby, J.E. Warren, CrystEngComm 7 (2005) 548.
[26] H.F. Clausen, R.D. Poulsen, A.D. Bond, M.-A.S. Chevallier, B.B. Iversen, J. Solid State Chem. 178 (2005) 3342.
[27] M. Bujak, R.J. Angel, J. Solid State Chem. 180 (2007) 3026.
[28] J. Yan, H. Zhao, Z. Li, Y. Xing, X. Zeng, M. Ge, S. Niu, J. Cluster Sci. 20 (2009) 717.
[29] Y. Shen, H. Jiang, Z. Chen, J. Org. Chem. 75 (2010) 1321.
[30] J. Martínez-Lillo, D. Armentano, T.F. Mastropietro, M. Julve, J. Faus, G. De Munno, Cryst. Growth Des. 11 (2011) 1733.
[31] J. Martinez-Lillo, D. Armentano, N. Marino, L. Arizaga, R. Chiozzone, R. Gonzalez, C. Kremer, J. Cano, J. Faus, Dalton Trans. (2008) 4585.
[32] X.-Y. Wang, L. Gan, S.-W. Zhang, S. Gao, Inorg. Chem. 43 (2004) 4615.
[33] X.-Y. Wang, H.-Y. Wei, Z.-M. Wang, Z.-D. Chen, S. Gao, Inorg. Chem. 44 (2005) 572.
[34] S.-R. Fan, L.-G. Zhu, Inorg. Chim. Acta 362 (2009) 2962.
[35] A. Plutecka, U. Rychlewska, Acta Crystallogr., Sect. C 65 (2009) m75.
[36] N.R. Kelly, S. Goetz, S.R. Batten, P.E. Kruger, CrystEngComm 10 (2008) 1018.
[37] H.L. Chen, Y. Ding, X.X. Xu, E.B. Wang, W.L. Chen, S. Chang, X.L. Wang, J. Coord. Chem. 62 (2009) 347.
[38] F.N. Shi, L. Cunha-Silva, T. Trindade, F.A.A. Paz, J. Rocha, Cryst. Growth Des. 9 (2009) 2098.
[39] T. Kajiwara, H. Wu, T. Ito, N. Iki, S. Miyano, Angew. Chem., Int. Ed. 43 (2004) 1832.
[40] Y.-F. Zhou, F.-L. Jiang, D.-Q. Yuan, B.-L. Wu, R.-H. Wang, Z.-Z. Lin, M.-C. Hong, Angew. Chem., Int. Ed. 43 (2004) 5665.
[41] B. Nohra, P. Mialane, A. Dolbecq, E. Riviere, J. Marrot, F. Secheresse, Chem. Commun. (2009) 2703.
[42] T. Yamaguchi, Y. Sunatsuki, M. Kojima, H. Akashi, M. Tsuchimoto, N. Re, S. Osa, N. Matsumoto, Chem. Commun. (2004) 1048.
[43] U. Abram, D.B. Dell'Amico, F. Calderazzo, C.D. Porta, U. Englert, F. Marchetti, A. Merigo, Chem. Commun. (1999) 2053.
[44] Y. Bretonniere, M. Mazzanti, J. Pecaut, F.A. Dunand, A.E. Merbach, Chem. Commun. (2001) 621.
[45] L. Canadillas-Delgado, O. Fabelo, J. Cano, J. Pasan, F.S. Delgado, F. Lloret, M. Julve, C. Ruiz-Perez, CrystEngComm 11 (2009) 2131.
[46] A. Rohde, W. Urland, Dalton Trans. (2006) 2974.
[47] K.G. Alley, A. Mukherjee, R. Clerac, C. Boskovic, Dalton Trans. (2008) 59.
[48] L.J. Charbonniere, S. Mameri, D. Flot, F. Waltz, C. Zandanel, R.F. Ziessel, Dalton Trans. (2007) 2245.
[49] D. John, W. Urland, Eur. J. Inorg. Chem. (2005) 4486.
[50] D. John, W. Urland, Eur. J. Inorg. Chem. (2006) 3503.
[51] S. Worl, I.O. Fritsky, D. Hellwinkel, H. Pritzkow, R. Kramer, Eur. J. Inorg. Chem. (2005) 759.
[52] G. Franc, C.-O. Turrin, E. Cavero, J.-P. Costes, C. Duhayon, A.-M. Caminade, J.-P. Majoral, Eur. J. Inorg. Chem. (2009) 4290.
[53] D. Guo, Y.-T. Li, C.-Y. Duan, H. Mo, Q.-J. Meng, Inorg. Chem. 42 (2003) 2519.
[54] R. Calvo, R.E. Rapp, E. Chagas, R.P. Sartoris, R. Baggio, M.T. Garland, M. Perec, Inorg. Chem. 47 (2008) 10389.
[55] Y. Bretonniere, M. Mazzanti, J. Pecaut, F.A. Dunand, A.E. Merbach, Inorg. Chem. 40 (2001) 6737.
[56] C.-B. Liu, X.-J. Zheng, Y.-Y. Yang, L.-P. Jin, Inorg. Chem. Commun. 8 (2005) 1045.
[57] A.M. Atria, R. Baggio, M.T. Garland, J.C. Munoz, O. Pena, Inorg. Chim. Acta 357 (2004) 1997.
[58] A. Rizzi, R. Baggio, M.T. Garland, O. Pena, M. Perec, Inorg. Chim. Acta 353 (2003) 315.
[59] Y. Cui, F. Zheng, Y. Qian, J. Huang, Inorg. Chim. Acta 315 (2001) 220.
[60] S. Aime, G. Bombieri, C. Cavallotti, G.B. Giovenzana, D. Imperio, N. Marchini, Inorg. Chim. Acta 361 (2008) 1534.
[61] S. Cotton, Lanthanide and Actinide Chemistry, John Wiley & Sons, West Sussex, 2006.
[62] A. Panagiotopoulos, T.F. Zafiropoulos, S.P. Perlepes, E. Bakalbassis, I. Masson-Ramade, O. Kahn, A. Terzis, C.P. Raptopoulou, Inorg. Chem. 34 (1995) 4918.
[63] J.-P. Costes, J.M. Clemente-Juan, F. Dahan, F. Nicodeme, M. Verelst, Angew. Chem., Int. Ed. 41 (2002) 323.
[64] Z.H. Zhang, Y. Song, T. Okamura, Y. Hasegawa, W.Y. Sun, N. Ueyama, Inorg. Chem. 45 (2006) 2896.
[65] H. Hou, G. Li, L. Li, Y. Zhu, X. Meng, Y. Fan, Inorg. Chem. 42 (2003) 428.
[66] A. Rohde, W. Urland, Dalton Trans. (2006) 2974.
[67] J. Curely, Europhys. Lett. 32 (1995) 529.
[68] J. Curely, J. Rouch, Phys. B-Condens. Matter 254 (1998) 298.
[69] L. Canadillas-Delgado, O. Fabelo, J. Pasan, F.S. Delgado, F. Lloret, M. Julve, C. Ruiz-Pérez, Dalton Trans. 39 (2010) 7286.
[70] J.P. Costes, J.M.C. Juan, F. Dahan, F. Nicodeme, Dalton Trans. (2003) 1272.
[71] L.E. Roy, T. Hughbanks, J. Am. Chem. Soc. 128 (2006) 568.
[72] R. Baggio, R. Calvo, M.T. Garland, O. Peña, M. Perec, A. Rizzi, Inorg. Chem. 44 (2005) 8979.